Mixed Regime Simulation in MEMS

by

Deepak Ramaswamy

Submitted to the Department of Civil and Environmental Engineering
in partial fulfillment of the requirements for the degree of

Master of Science

at the

MASSACHUSETTS INSTITUTE OF TECHNOLOGY

May 1998

Author ....
Department of Civil and Environmental Engineering
May 8, 1998

Certified by..... .....
Jacob White
Professor of Electrical Engineering and Computer Science
Thesis Supervisor

Certified by.. .....
Kevin Amaratunga
Assistant Professor of Civil and Environmental Engineering
Thesis Reader

Accepted by..... .....
Joseph M. Sussman
Chairman, Department Committee on Graduate Students

Mixed Regime Simulation in MEMS

by

Deepak Ramaswamy

Submitted to the Department of Civil and Environmental Engineering
on May 8, 1998, in partial fulfillment of the
requirements for the degree of
Master of Science

Abstract

In order to verify and optimize the performance of MEMS devices, simulators are required which can rapidly analyze complicated three dimensional structures. One approach to improving simulation speed is to develop techniques which allow designers to improve simulation efficiency by using simpler physical approximations in parts of the device. Here,such a mixed regime approach is described to accelerating a matrix-implicit multi-level Newton method for electromechanical simulation. In particular, a general algorithm is described which allows parts of the mechanical structure to be approximated as as rigid, as each rigid body contributes only six degrees of freedom. Results are presented to show that the method can perform accurate 3-D simulation of a complete electrostatic comb drive accelerometer in under ten minutes.

Thesis Supervisor: Jacob White
Title: Professor of Electrical Engineering and Computer Science

Acknowledgments

First of all I would like to thank my advisor Professor Jacob White for his deep insight, direction and help on the theoretical and implementation aspects he provided throughout my research. I would also like express my thanks for Narayan Aluru for helping me out on the finite element elastostatics and coupled domain simulation aspects of my research. I would like to very much acknowledge the help I received from my group mates at various stages of my research. Finally I wish to express my thanks towards Professor Kevin Amaratunga who read this thesis and suggested corrections while pointing out mistakes. .

Contents

List of Figures

Chapter 1

Introduction

A MEMS structure often consists of a behaviorally rigid part and an elastic part even though it is built from a single material. Therefore, it is possible to model part of the structure as rigid for a rapid self-consistent electromechanical analysis (Senturia et al [8]). An example of such a structure is shown in Figure 1-1.

One approach to reducing the high computational cost of coupled electromechanical simulation of three dimensional micro-electro-mechanical devices is to allow designers to use rigid body approximations where appropriate.

The cube structure in the center of the comb drive mentioned before is known as the proof mass supported by tethers at two ends and is largely rigid. Figure (1-2) shows the reduction of the original finite element matrix on the left to the reduced

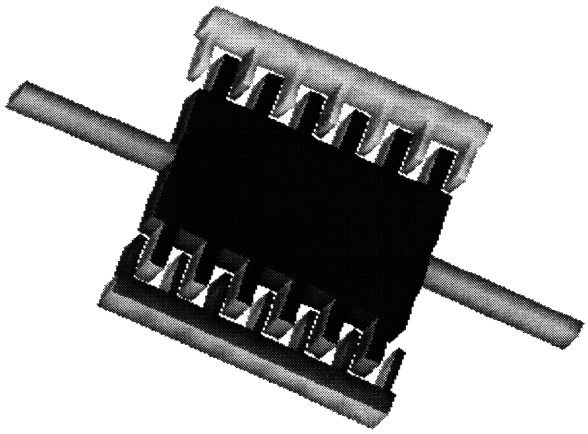

Figure 1-1: Comb Drive Accelerometer

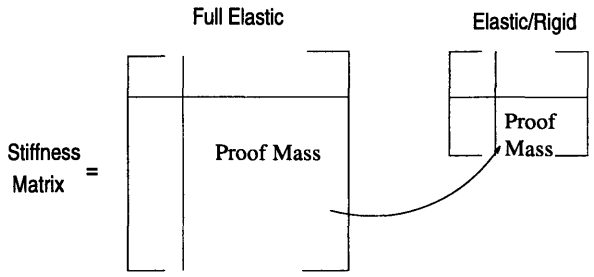

Figure 1-2: Matrix size reduction

matrix on the right.

To gain from such an approach, it is essential that the mixed-regime rigid-elastic system be constructed automatically and simulated efficiently. Chapter 2 describes three efficient rigid body formulations. Chapter 3 describes both how to extract rigid bodies given an input file of elements , and how to efficiently construct the rigid-elastic system stiffness matrix, gives a brief background in finite-element elastostatic analysis, presents one coupled domain simulation method and addresses other formulations.

In chapter 4 computational results are presented demonstrating that the rigid-elastic simulator is more than 300 times faster than a purely elastic simulator for a comb-drive problem. Finally, it is demonstrated that the mixed-regime simulator can be used as part of a coupled-domain simulator to perform 3-D electromechanical analysis of an entire comb drive in under ten minutes.

Chapter 2

Formulation

A rigid body requires only six variables to represent it, namely the three rotation parameters [4], [3] and the three translation parameters. However it can be formulated in terms of parameters greater than six. For a rigid body motion $x \rightarrow y$ of a body B the position of any *material* point X of $\mathcal{B}$ in the current or deformed configuration, y is expressed as

$$y = Rx + c \tag{2.1}$$

where x is the position of X in the reference or original configuration, R an orthogonal tensor and c a translation are constant for all X. Therefore we have

$$RR^T = I \tag{2.2}$$

Here three approaches to the parameterization of the rigid body are considered.

2.1 Representation of R

2.1.1 Euler angles approach

R is represented in terms of the *Euler* angles ϕ, ψ and θ as being

$$R = \begin{bmatrix} \cos\phi\cos\psi - \sin\phi\sin\psi\cos\theta & -\cos\phi\sin\psi - \sin\phi\cos\psi\cos\theta & \sin\psi\sin\theta \\ \sin\phi\cos\psi + \cos\psi\sin\psi\cos\theta & -\sin\phi\sin\psi + \cos\phi\cos\psi\cos\theta & -\cos\phi\sin\theta \\ \sin\psi\sin\theta & \cos\psi\sin\theta & \cos\theta \end{bmatrix} \tag{2.3}$$

We note that R is singular for $\theta = \phi = \psi = 0$.

The *Euler* angles represent rotations about a set of three orthogonal axes. Denoting the orthogonal basis in $\Re^3$ as e_1, e_2 and e_3 and the original configuration as X, θ would denote a rotation about e_3 leading to a configuration X'. ψ then defines a rotation about e_2 in X' leading to a configuration X''. In X'' then, the axes are rotated about e_1 with an angle of ϕ. The point to note is that while the axes have undergone an orthogonal transformation, when the body is rigid, a point on that body has *not* undergone any deformation with respect to the rotated axes. Therefore the position y of the point on the rigid body is a function only of the *Euler* angles in addition to the translation.

The rigid body is then parameterized by a total of six variables.

2.1.2 Quaternion approach

Quaternions are essentially a generalization of complex numbers and represents simply another group theory. A quaternion q is defined as an ordered set of four real numbers

$$q = (w, x, y, z) \tag{2.4}$$

with the following rules of addition and multiplication if $q' = (w', x', y', z')$ then

$$q + q' = (w + w', x + x', y + y', z + z') \tag{2.5}$$

$$qq' = (ww' - xx' - yy' - zz', wx' + xw' + yz' - zy', wy' - xz' + yw' + zx', wz' + xy' - yx' + zw') \tag{2.6}$$

The quaternion $(k, 0, 0, 0)$ represents a *real* number k. The conjugate $\overline{q}$ is defined as

$$\overline{q} = (w, -x, -y, -z) \tag{2.7}$$

$(0, x, y, z)$ is a quaternion analogue of the imaginary part of a complex number. quaternions can also be thought of as

$$q = (s, v) \tag{2.8}$$

where s is a scalar and v is a three dimensional vector. Writing q in terms of an orthogonal basis i, j, k

$$q = s + ai + bj + ck \tag{2.9}$$

The unit quaternion is then $\hat{q} = \frac{q}{\sqrt{s^2+a^2+b^2+c^2}}$ where the denominator is $\sqrt{q\overline{q}}$, a definition for a norm of q. Denoting $\cos\theta = \frac{s}{\sqrt{s^2+a^2+b^2+c^2}}$ and $\sin\theta = \frac{\sqrt{a^2+b^2+c^2}}{\sqrt{s^2+a^2+b^2+c^2}}$ we have

$$\hat{q} = \cos\theta + \sin\theta v \tag{2.10}$$

where $v = \frac{0+ai+bj+ck}{\sqrt{a^2+b^2+c^2}}$ is a unit *vector*.

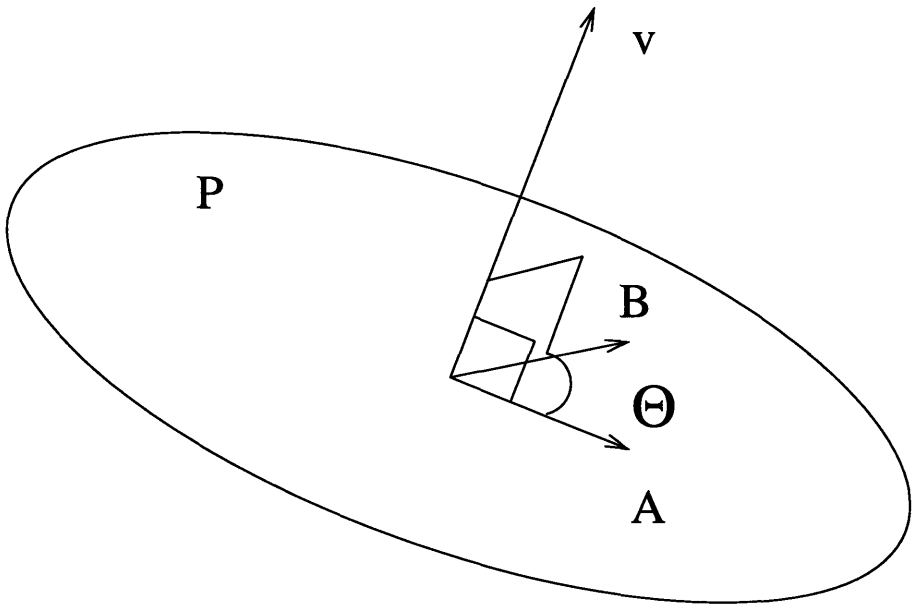

Figure 2-1: Rotation operation

Quaternion operator

From the figure, we observe that the operator $\hat{q}$ when it operates on quaternion A produces B (note that their scalar terms are zero). Therefore

$$B = \hat{q}A \tag{2.11}$$

This allows for a four term parametrization of R as any rotation of $\mathcal{B}$ can be thought of in terms of a spin *direction* (a,b,c) and a spin *angle* (θ) or in other words $\hat{q}$.

2.1.3 Orthogonal tensor approach

In this approach R is simply represented as

$$R = \begin{bmatrix} a & b & c \\ d & e & f \\ g & h & i \end{bmatrix} \tag{2.12}$$

2.2 Rigid Body equations

2.2.1 Euler Angles

The six equations of static force and moment equilibrium of the rigid body match the six parameters here. Namely

$$F_x = F_y = F_z = M_x = M_y = M_z = 0; \tag{2.13}$$

where $M_{x,y,z}$ represent the components of the moment vector along the x, y and z axes at some point about which equilibrium is determined.

2.2.2 Quaternion

In addition to the equations of equilibrium, we have the condition

$$\hat{q}\bar{\hat{q}} = 1 \tag{2.14}$$

Therefore we have seven variables including the three translation components and seven equations.

2.2.3 Orthogonal tensor

From equation, we have

$$\begin{bmatrix} a & b & c \\ d & e & f \\ g & h & i \end{bmatrix} \begin{bmatrix} a & d & g \\ b & e & h \\ c & f & i \end{bmatrix} = \begin{bmatrix} 1 & 0 & 0 \\ 0 & 1 & 0 \\ 0 & 0 & 1 \end{bmatrix} \tag{2.15}$$

Noting that RR^T is symmetric, we have six equations from above in addition to the six equilibrium equations for the twelve variables that we have here which is inclusive of the three translation components.

Chapter 3

Rigid Bodies Assembly and FE-Rigid Bonding

3.1 Assembly

Any sort of scheme or code which seeks to recognize that certain elements of the structure behave rigidly should be able to do just that in an efficient manner. If the stiffness matrix is large in some norm then the element could be classified as rigid. However it is important to note that it is the relative stiffness of elements and the nature and magnitude of the load which determine the rigid behavior of an element. If apriori it is known which elements behave rigidly then we could for example give those elements a very high modulus of elasticity and then perform an assembly of rigid elements after the input of structure geometry and loading. The assembler should be able to recognize for example (although unlikely to occur in practice) the case as shown in Figure 3.1.

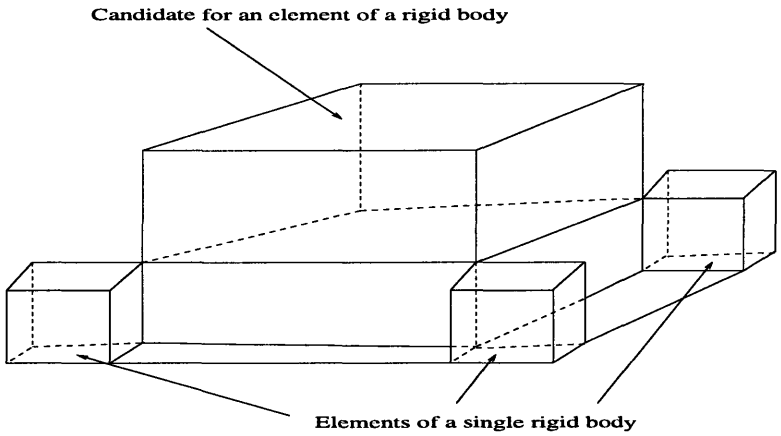

Figure 3-1: Rigid body assembly

3.1.1 Assembly algorithm

If K denotes the number of elements and the $\mathcal{R}$ denotes the set of the rigid elements then the assembly algorithm is written as

$\forall\ i = 1\ to\ K$
  $if\ material\ (i) = \infty\ and\ i \notin \mathcal{R}$
    $\mathcal{R} = \mathcal{R} \cup i$
    $\forall\ j \in neighbors\ (i)$
      $if\ material\ (j) = \infty$
        $\mathcal{R} = \mathcal{R} \cup j$
      end
    end
  end
end

Let us examine Figure 3.2 which depicts the assembly of two dimensional elements. First element 1 is identified as rigid as its elastic modulus is very large and incorporated into rigid body say R_1. Then 1's neighbors are examined and 2,3,6 and 7 are determined as rigid. However 3, 6 and 7 are connected through one point only to 1 and are hence not elements of R_1 yet. Therefore 2 which satisfies this criterion is now part of R_1. The arrows show the building of R_1 through addition of elements

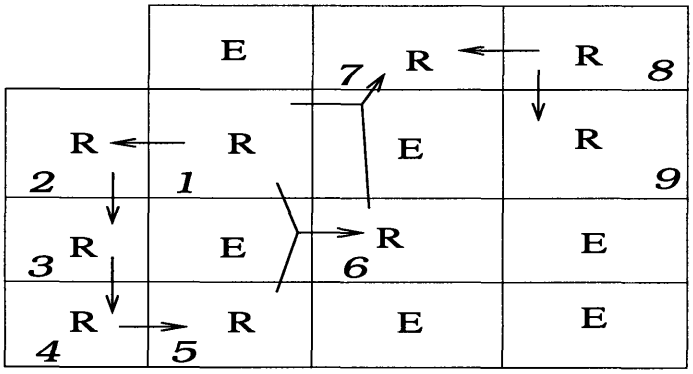

R - Rigid Element , E - Elastic Element

Figure 3-2: Rigid body assembly

2 through 5. 5's rigid neighbor 6 is connected to it through only one node but now 6 is now *connected to* R_1 through 2 nodes and therefore 6 is assimilated into R_1. $R_1 = 1, 2, 3, 4, 5, 6$. Since R_1 is locally "complete", R_2 is assembled in a similar way. $R_2 = 7, 8, 9$. However now R_1 and R_2 are connected through 2 nodes. Therefore $R_1 = R_1 \cup R_2$.

We note that if 6 were connected to R_1 through only one node then the entire rigid body formulation would fail because the force exerted between 1 and 6 would be indeterminate. We also note that the rigid body connection requirement in 3-D would be at least three noncollinear nodes.

This depth first algorithm is most efficient for structures which have clustered rigid elements. For otherwise a breadth first algorithm will be more efficient.

3.2 Finite Element formulation

Referring to [2] a total Lagrangian representation is adopted in which the finite element volume integrations are carried out with respect to the original configuration. For quasi-static analysis, the Newton method is written as

$$\int_{Vo} C_{ijrs}^{k-1} \Delta e_{rs}^{k} \delta e_{ij} dV + \int_{Vo} S_{ij}^{k-1} \delta \Delta \eta_{ij}^{k} dV = \Re - \int_{Vo} S_{ij}^{k-1} \delta \epsilon_{ij}^{k-1} dV \qquad (3.1)$$

where C_{ijrs} is the right Cauchy-Green deformation tensor, S_{ij} the second Piola-

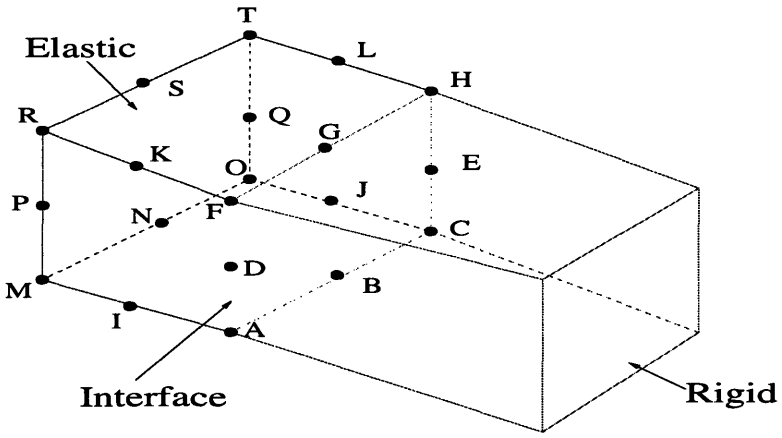

Figure 3-3: FE-Rigid Interface

Kirchhoff stress tensor, ϵ_{ij} the Green-Lagrange strain tensor, e_{ij} is the small strain tensor and $\eta_{ij} = \epsilon_{ij} - e_{ij}$. All quantities inside the volume integral are referred to in the original configuration.

In the final finite element formulation the Newton method is

$$(K_L + K_{NL})U = \Re - F \tag{3.2}$$

where $\Re$ is the externally applied nodal load vector, F is the equivalent internal nodal force vector, K_L is the linear stiffness matrix, K_{NL} is the nonlinear stiffness matrix, and U is the displacement vector. In this study only geometric nonlinearity and not material nonlinearity has been considered as materials such as PolySilicon often used in MEMS are linearly elastic.

20 node parabolic brick elements were considered and the total Lagrangian method of analysis was used.

3.3 Finite element-Rigid Bonding

Figure 3.3 shows a 20 node finite element interface with a rigid element. We note that a rigid element has a need for interface nodes only for communicating the displacement conditions at the interface with the finite element. The stiffness matrix or Jacobian for the elastic element shown will have components due to the rigid body parameters

and the forces acting at A through H on the rigid body will be a function of nodes I through T. Therefore the Jacobian for the force equilibrium function for the rigid body will have components, in this case, due to the displacement variables at the physical nodes I through T.

Representing the rigid body through Euler angles, the equilibrium equation is

$$F(\vec{u}, \theta, \phi, \psi, xR, yR, zR) = 0 \tag{3.3}$$

Assuming a convenient ordering of the Jacobian,

$$J_F = \begin{bmatrix} K_{EE} & K_{ER} \\ K_{RE} & K_{RR} \end{bmatrix} \tag{3.4}$$

- K_{EE} is the elastic - elastic interaction. This is simply the sum of the K_{NL} and K_L matrices mentioned in the the finite element formulation section excluding the entries due to the interface nodes.

- K_{ER} is the elastic - rigid interaction. We have for node variables x_i $(i = A..H)$ on the interface

$$\frac{\partial F}{\partial \theta} = \frac{\partial F}{\partial x_A}\frac{\partial x_A}{\partial \theta} + \frac{\partial F}{\partial x_B}\frac{\partial x_B}{\partial \theta} + \cdots + \frac{\partial F}{\partial x_H}\frac{\partial x_H}{\partial \theta} \tag{3.5}$$

  Here the chain rule has been applied.

  and we have

$$x_i = x_i(\theta, \phi, \psi, xR, yR, zR) \tag{3.6}$$

  from the rigid body formulation.

- K_{RE} , the rigid - elastic term is present because the equivalent nodal forces on the interface with the rigid body are dependent on the variables associated with nodes $I..T$ of the elastic element and these forces contribute in the equilibrium

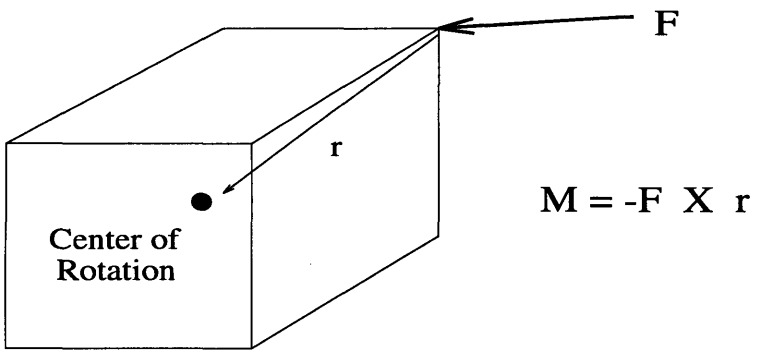

Figure 3-4: Determining Moment

of the rigid body. For example the Moment M of the rigid body is

$$M = L(F_i^I) \tag{3.7}$$

where L is an operator linear in F_i^I, a interface nodal force component. Then

$$\frac{\partial M}{\partial x} = L(\frac{\partial F_i^I}{\partial x}) \tag{3.8}$$

but $\frac{\partial F_i^I}{\partial x}$ is directly obtained from K_{EE}.

The only forces in the rigid/elastic interface are the equivalent nodal forces and it is important to realize that these elastic force projections are such that the virtual work on the element due to them equals the virtual work due to element internal stresses and are therefore not an exactly equivalent force system to the interface surface pressure exerted by the elastic element on the rigid element.

- K_{RR} is the purely rigid-rigid interaction term. This term arises from the external pressure and point loads on the rigid body. In case of pressure forces such as that due to a fluid, the force is always normal to the surface of the body. As a result thereof the pressure is geometry dependent and hence its contribution to J and specifically K_{RR} must be computed. To see this clearly lets examine the following figure. Let vectors $\xi_1 ... \xi_4$ in Euclidean space define a rectangular rigid body surface with $||\ ||$ denoting the standard Euclidian norm and let the

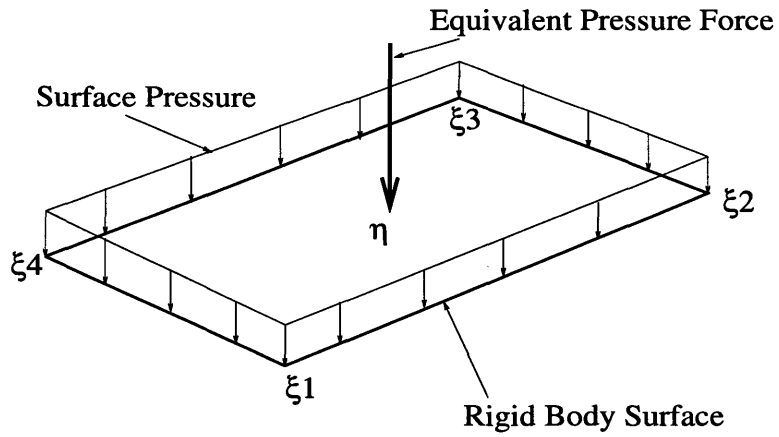

pressure acting normally on the surface have a constant magnitude p. Then the equivalent force system F acting on the surface acts at the center of mass of the surface $\eta = (\xi_1+\xi_2+\xi_3+\xi_4)/4$ with $\|F\| = p\,\|\xi_1-\xi_2\|\,\|\xi_2-\xi_3\|$. Note $\|F\|$ is independent of the rigid body parameters as the surface doesn't stretch . However the direction of F is along $\hat{n} = \pm\frac{(\xi_1-\xi_2)\ X\ (\xi_2-\xi_3)}{\|(\xi_1-\xi_2)\ X\ (\xi_2-\xi_3)\|}$. Additionally lets denote the center of rotation as χ. F then is the contribution to the equation $\mathcal{F} = 0$ and the contribution to $\mathcal{M} = 0$ is $F\ X\ (\eta-\chi)$ or $\|F\|\ \frac{(\xi_1-\xi_2)\ X\ (\xi_2-\xi_3)}{\|(\xi_1-\xi_2)\ X\ (\xi_2-\xi_3)\|}\ X\ (\eta-\chi)$. Note that $\xi_i = f(\chi, R)$ where R is the rotation tensor. Therefore $\mathcal{M}$ contributes to K_{RR}.

3.4 Asymmetry of J

This formulation is essentially black box in nature as it retains the original finite element assembly algorithm. It is to be noted that the interface A - H always retains its original configuration. It is also clear that only Dirichlet boundary conditions can be prescribed on the rigid body. However we note that the symmetry of the original Jacobian has been destroyed as the rigid body formulation is not symmetric.

3.5 Self-Consistent Coupled Simulation

3.5.1 Multilevel Newton

For a selfconsistent coupled simulation, the rigid/elastic formulation is coupled with the precorrected FFT accelerated electrostatic solver [5] in a multilevel Newton method [6]. If we think of the electrostatic and mechanical solvers as being black boxes returning

$$q = H_E(u) \tag{3.9}$$

and

$$u = H_M(q) \tag{3.10}$$

The Newton method is therefore

$$\begin{bmatrix} I & -\frac{\partial H_E}{\partial u} \\ -\frac{\partial H_M}{\partial q} & I \end{bmatrix} \begin{bmatrix} \Delta q \\ \Delta u \end{bmatrix} = - \begin{bmatrix} q - H_E \\ u - H_M \end{bmatrix} \tag{3.11}$$

The above system is solved using matrix free GMRES and the matrix vector product is determined with black box calls to individual solvers. Already block preconditioned, multilevel Newton has better global convergence but is slower than full Newton [6], [8].

3.6 Issues in formulation

The three formulations in chapter 2 were implemented for simple problems involving struts and joints and a single rigid body. It was experimentally determined that the formulation involving Euler angles converged most often and in fewer number of iterations. The reason for this is explained as follows. The formulation involving Euler angles always preserves the geometry of the rigid body as the cosines and sines of the angles are bounded. But the quaternion formulation does not perforce maintain the rigid body geometry as the only the spin is bounded. In fact the explicit tensor formulation easily performs the worst. This being case the Euler angle formulation

was adopted into the Galerkin finite element formulation.

3.7 Other methods for representing rigid bodies

The orthogonal deformation constraint can be added via Lagrange multipliers to the original variational formulation. However this implies that for every position which is constrained we would have one multiplier and therefore this would lead to a very large linear system.

The imposition of the rigid body deformation as a boundary condition in a Galerkin based variational method is also not direct because the set of orthogonal rotations do not form a linear space , namely $R_1, R_2 \in X$ where X is the space of orthogonal tensors does not $\Rightarrow R_1 - R_2 \in X$ and therefore the solution space cannot be represented by a basis.

Imposition of the rigid body constraint could be also thought of in postprocessing terms i.e. given

$$KU_{master} = F \tag{3.12}$$

where K is the "full elastic" stiffness matrix , U_{master} the original set of variables and F the forcing term, we could have a transformation Q such that

$$U_{master} = QU_{slave} \tag{3.13}$$

where U_{slave} is the reduced set with both rigid body and elastic variables. Therefore

$$KQU_{slave} = F \tag{3.14}$$

which implies

$$Q^T KQU_{slave} = Q^T F \tag{3.15}$$

with $Q^T K Q$ being a reduced matrix. However a form of Q which operates linearly on U_{slave} cannot be obtained by expressing R in terms of the Euler angles because of the dependence of R on cosines and sines.

3.8 Stress singularity

The elastic/rigid interface might experience strong stress jumps because the rigid body is essentially being constrained not to change shape. Therefore if the actual elastic stiffness is not infinitely large at a point on the rigid body the stress is zero since the strain is zero. Instead a scheme could be configured , in the comb drive for example, in which the rigid block lies in the interior of the proof mass surrounded on all sides by a boundary of elastic elements.

Chapter 4

Results

4.1 Mechanical Solver

Testing the mechanical solver alone, the fingers and the tethers were taken as elastic and the CPU time was determined with varying the number of fingers each of which had 2 brick elements as shown in Figure 4-1. The tethers each had 3 brick elements. Random loads were applied on the surfaces of the elements of the proof mass.

The CPU time plotted against the mesh density of the rigid proof mass is shown in Figure 4-2

The dip in the CPU time is explained by the fact that random loads are applied and that Newton's method is sensitive to applied loads. We observe that the overall

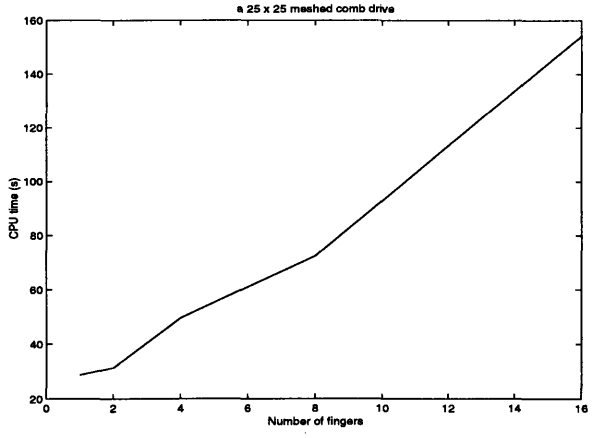

Figure 4-1: Number of Fingers Vs CPU time

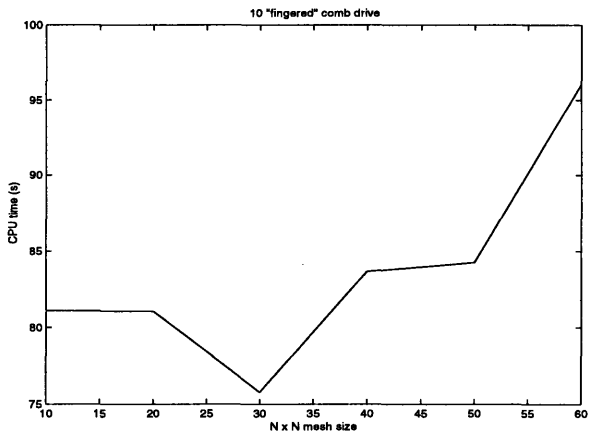

Figure 4-2: Proof Mass Mesh Size Vs CPU time

CPU time for the second case is less than and is not as sensitive as that for the first case. This is to be expected as increasing the mesh size does not increase the number of degrees of freedom of the proof mass which remains fixed at six. The CPU time slightly increases because there are more discrete surfaces on the rigid body to perform operations over.

4.2 Simulation Results

The comb drive accelerometer shown in Figure 1-1 was tested using a mixed rigid/elastic formulation on a DEC Alpha 433 MHz. The proof mass and fingers were taken as rigid and the tethers were elastic. The material was polysilicon. The proof mass has a dimension of 100 X 100 X 10 , the tethers 60 X 10 X 10 and the fingers 30 X 10 X 10. There is no ground plane.

4.2.1 Mechanical only simulation

The CPU time required for the mechanical linear system solve for the rigid/elastic case is 55.63 ms whereas it is 21,628.15 ms for the full elastic simulation.

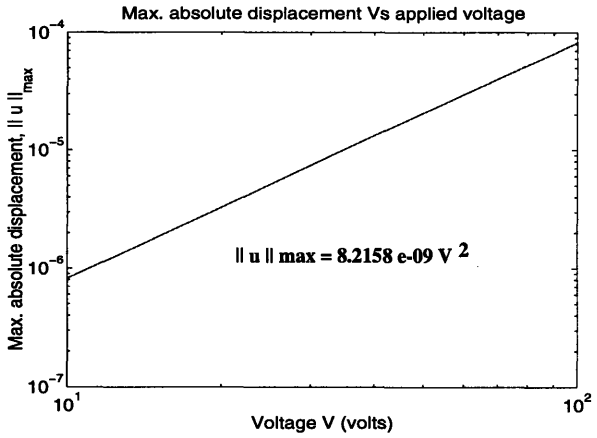

Figure 4-3: Maximum displacement Vs applied voltage

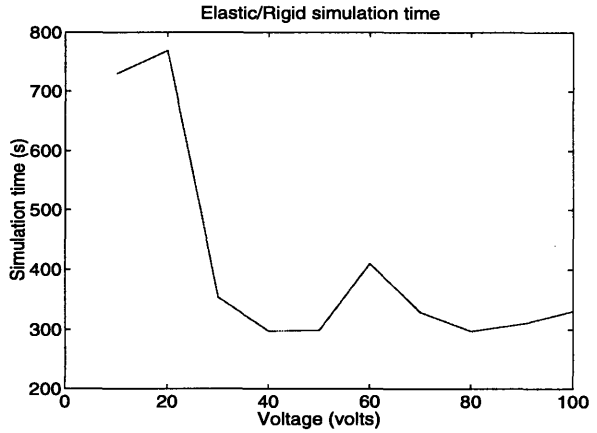

Figure 4-4: Rigid/Elastic Coupled Simulation

4.2.2 Coupled electromechanical simulation

The mixed regime mechanical simulator was then combined with the precorrected FFT accelerated electrostatic solver [5] using the multilevel Newton method [6]. Figure 4-3 shows the nonlinear variation of the output functional taken to be the maximum absolute displacement, becoming increasingly stiff with increasing voltage, v on one of the supports of the structure. The central structure and the other support were kept at 0 volts. The CPU time for this coupled-domain mixed-regime simulation is plotted as a function of applied voltage in Figure 4-4. Note that computing the displacement for a given voltage takes less than ten minutes.

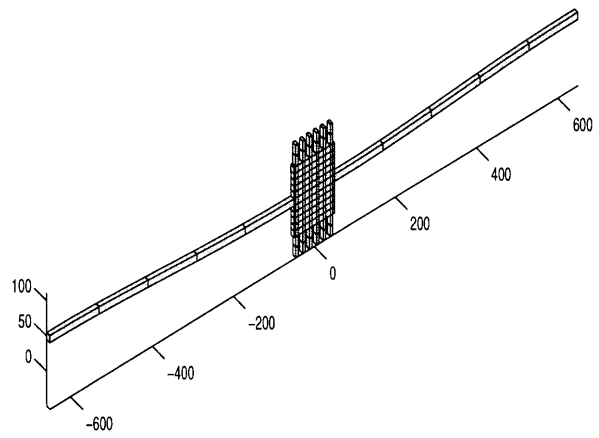

Figure 4-5: Long tethered comb with displacement 0.75 microns under 10 V

Chapter 5

Conclusion

A mixed rigid/elastic formulation leads to a considerable saving in the mechanical solver computation time requiring at the same time much less memory than a full elastic analysis. With an automation of the rigid element identification process, this leads to an efficient coupled electromechanical analysis.

Bibliography

[1] N.R. Aluru and J. White. Direct-newton finite element/boundary-element technique for micro-electro-mechanical analysis. Tech. digest, solid-state sensor and actuator workshop, Transducers Research Foundation, Cleveland Heights, Ohio, 1996.

[2] K. J. Bathe. *Finite Element Procedures.* Prentice-Hall Inc., Englewood Cliffs, NJ, 1996.

[3] P. Chadwick. *Continuum mechanics.* Halsted Press, New York, 1976.

[4] Morton E. Gurtin. *An introduction to continuum mechanics.* Academic Press, New York, 1981.

[5] J.R. Phillips and J. K. White. *Precorrected-FFT Methods for Electromagnetic Analysis of Complex 3-D Interconnect and Packages*, Proc. PIERS '95, Progress in Electromagnetic Research Symp., 1995.

[6] N.R. Aluru and J. White. *A Coupled Numerical Technique for Self-Consistent Analysis of Micro-Electro-Mechanical Systems*, volume 59 of *Microelectromechanical Systems (MEMS), ASME Dynamic Systems and Control (DSC) series : Proc. 1996 ASME Int'l Mechanical Engineering Congress and Exposition*, New York, 1996.

[7] S.J. Sherman, W.K. Tsang, T.A. Core, D.E. Quinn. *A low cost monolithic accelerometer*, 1992 Symposium on VLSI Circuits. Digest of Technical papers, 1992.

[8] Narayan Aluru Stephen D. Senturia and Jacob White. Simulating the behavior of mems devices: Computational methods and needs. *IEEE Computational Science and Engineering*, 4(1):30–43, jan-mar 1997.